on the order of 0.05, which gives a value of $(\rho_a/\rho_j)$ below that for the experiments in Figure 2. On this basis there should be no observed effect in the truly turbulent case either.

## CONCLUDING REMARKS

The experiments herein reported show that the analysis given in the preceding paper, Phinney (1973), was incomplete. In Figure 5 of that paper, what was purported to be the influence of the ambient Weber number $We_a$ on breakup length should be interpreted as the variation due to the jet Weber number $We_j$. The failure to be able to distinguish between the two parameters was due to the fact that almost all of the data were taken with the jet fluid being water and the ambient gas being atmospheric air. The new experiments suggest the necessity of an additional breakup mechanism that was not considered in the previous paper. The new parameter can be thought of as representing a new mode of breakup, although it reduces to $We_j$ which governs pseudo laminar breakup (with no ambient influence) as well. A large portion of the existing experimental data is in the range of this new mode of breakup. The pseudo laminar breakup that was described in the previous paper does appear to be a valid picture of the breakup of turbulent jets with low enough exit velocity, $\sqrt{We_j} < 25$. The influence of the ambient atmosphere was not observed, although it should be present in either mode of breakup if the ambient density is high enough.

The remarks in the previous paper, Phinney (1973), concerning the optical observations of breakup still stand and are consistent with the present work. Near the exit, the turbulent motion produces protuberances which give the surface a rough spiky appearance. Since the surface tension force normal to the surface is inversely related to the radius of curvature, the sharper the protuberance the more strongly it is contained. For this reason, it is likely that at low velocity, where the turbulent motion is only somewhat above the threshold, the ultimate breakup of the jet will be due to fairly long wavelength disturbances just as in the case of pseudo laminar breakup. General observations show that as the exit velocity is increased (and the turbulent intensity becomes higher), the breakup becomes more violent and the scale and droplet size decrease.

The statistical measurements that were presented in Figure 6 of the previous paper span the range from the pseudo laminar to the truly turbulent. In particular, the low Reynolds number runs for cases *CI* and *DI* are just below the break in the curves; case *BI* ($Re = 8500$) is at the break, and all the rest are at some point above the break. All these data seem to correlate in terms of the parameters in that figure.

Although the present data did not show an ambient density influence, there must be a threshold above which this effect exists and could be studied. It would be useful to perform these additional experiments. Unfortunately, because of the design of the apparatus, it was not possible to pressurize it, thus making the higher range of $We_a$ inaccessible.


## ACKNOWLEDGMENT

This work was sponsored by the Chief of Naval Material under task number MAT-03L-000/ZR000-01-01 problem 193.


## NOTATION

$D$ = nozzle diameter
$I$ = turbulence intensity, $v_i/V$
$L$ = jet breakup length
$Re$ = jet Reynolds number, $\rho_j V D/\mu$
$v_i$ = root-mean-square value of a velocity typical of the jet internal motion
$V$ = mean jet exit velocity
$We_a$ = ambient Weber number, $\rho_a V^2 D/\sigma$
$We_j$ = jet Weber number, $\rho_j V^2 D/\sigma$
$\mu$ = viscosity coefficient of jet fluid
$\rho_a$ = density of ambient gas
$\rho_j$ = density of jet fluid
$\sigma$ = surface tension

## LITERATURE CITED


Chen, T. F., and J. R. Davis, "Disintegration of a Turbulent Water Jet," *Proc. Am. Soc. Civil Eng.*, **HY1**, 175 (1964).

Fenn, R. W., and S. Middleman, "Newtonian Jet Stability: The Role of Air Resistance," *AIChE J.*, **15**, 379 (1969).

Grant, R. P., and S. Middleman, "Newtonian Jet Stability," *AIChE J.*, **12**, 669 (1966).

Phinney, R. E., "The Breakup of a Turbulent Jet in a Turbulent Jet in a Gaseous Atmosphere," *JFM*, **60**, 689 (1973).



*Manuscript received April 2, 1975; revision received and accepted June 11, 1975.*


# Transient Viscoelastic Flow of Polymer Solutions


**Stress growth and stress decay data for two highly viscoelastic polymer solutions indicate that the first and second normal stress differences grow and decay at the same relative rates. These shear stress and first normal stress difference data are not represented well by the Spriggs, Bogue-Chen, or Carreau constitutive equations. The second normal stress difference, stress growth, and decay data are the first to be reported. The data were derived from radial pressure distributions and total normal and tortional forces obtained in cone and plate shearing. Sensitive miniature pressure transducers with pressure sensing diaphragms mounted flush with the plate surface provided the radial pressure distribution data.**



**W. R. LEPPARD**

**and**

**E. B. CHRISTIANSEN**

**Department of Chemical Engineering**
**University of Utah**
**Salt Lake City, Utah 84112**

W. R. Leppard is with Exxon Research and Engineering Co., Linden, New Jersey.

## SCOPE

The engineer involved in the design of polymer process equipment or in the interpretation of polymer flow experiments must have available reliable and accurate design or constitutive equations capable of describing steady flow and time dependent viscoelastic behavior. At least in simple shearing viscoelastic flow, the stress state is defined by the shearing stress and the first and second normal stress differences, $N_1$ and $N_2$. At present an equation or theory capable of describing the necessary time dependent stresses does not exist. However, there are several promising recent theories which approximately describe some simple time-dependent flows (Carreau, 1972; Spriggs, 1965; Chen and Bogue, 1972). The evaluation of such theories requires a comprehensive body of steady state and transient data. Unfortunately, most existing data are severely limited. Important limitations are the lack of unsteady flow, second normal stress difference data and the scarcity of accurate steady flow, second normal stress difference data. Also, accurate first normal stress difference data are not abundant. While $N_2$ is relatively small ($N_2/N_1 \cong -0.1$ to $-0.4$), there is evidence that it is important in some flow instabilities and in such operations as wire coating. The first normal stress difference is a measure of elasticity which is important, particularly in unsteady flows. The objective of this work is to provide a necessary set of data and to evaluate some constitutive equations. Complete stress state data for a 3% polyethylene oxide solution and a 2.5% polyacrylamide solution were obtained for stress growth and decay and for steady state and oscillatory shearing by means of a Model R-17 Weissenberg Rheogoniometer with cone and plate shearing geometry. This report is concerned with the stress growth and decay results; the oscillatory shearing studies have been previously reported (Christiansen and Leppard, 1974). Stress growth data consist of the stress vs. time trace from the instantaneous onset of shearing to the establishment of steady state. Stress decay data consist of the stress dependency on time from the abrupt termination of steady state shearing to the more or less complete decay of the stresses. The unique feature of this research is the use of very accurate, rapid response, miniature pressure transducers to measure the radial pressure distribution on the plate. The virtue of this instrumentation is that it makes possible the simultaneous measurement of data for computing the shear stress and $N_1$ and $N_2$ for transient and steady state conditions. The determination of transient $N_2$ data by previously used instrumentation is next to impossible, and such data have not been reported by other laboratories. Additionally, pressure distribution data together with the total normal force data from a single experiment provide for the computation of both $N_1$ and $N_2$ by independent means. The transducers were mounted with the 0.1 cm O.D. pressure sensing surface flush with the plate surface to preclude hole errors which have been a problem in much previous research. Furthermore, this instrumentation eliminates the need for a total axial thrust measurement, thus simplifying basic instrument design and, in principle, eliminating axial instrument compliance. Thus, with our instrumentation, the stress state of the fluid can be completely, accurately, and conveniently characterized during steady state and simple transient shearing.

## CONCLUSIONS AND SIGNIFICANCE

In the analysis of stress growth and decay data, it is convenient to use the normalized stress which is the ratio of the instantaneous stress to the steady state stress. It was observed that the normalized point stresses grew and decayed at the same rate independent of radial position. This observation makes possible a convenient means for the determination of transient, second normal stress differences from point stress data. It was demonstrated that since the normalized point stresses grew and decayed at the same rate, the related normalized first and second normal stress differences also grew and decayed at the same rate. These observations suggest a common origin for the first and second normal stress differences. Furthermore, if these observations prove generally valid, one need determine stress growth and decay data for only the most conveniently measured parameter, say the total normal force, and then compute other stress growth and decay data from these and the pertinent steady state data.

During stress development, both the shear and normal stresses and the normal stress differences overshot but did not undershoot their steady shear values at the shear rates investigated. The shear rates employed may have been too low to generate the stress undershoot reported by some researchers (see, for example, Laufer et al., 1973, Chen and Bogue, 1972). The overshoot was sooner and was of higher magnitude the higher the shear rate. The normalized normal stresses grew more slowly and exhibited a lower overshoot magnitude than did the normalized shear stresses. The stress decay studies indicate that the stresses decay more rapidly the higher the shear rate and that the shear stresses decay more rapidly than the normal stresses. These stress growth and decay observations are in qualitative agreement with previous experimental results and with the predictions of many constitutive relations (see, for example, Chen and Bogue, 1972, and Bird et al., 1974). The data reported represent the first set which has included stress growth and decay data for the second normal stress difference.

Three recent constitutive theories, the Spriggs, the Carreau, and the Bogue-Chen, are compared with the data. None describes the data well; however, the Carreau model is somewhat better overall.

---

One of the important requirements of a useful constitutive theory is that it adequately predict transient responses in simple geometrical flows. Such a requirement is particularly necessary in such viscoelastic flows as in some polymer processing operations, where the flows are transient and of short time spans. In consequence of recent progress, there are at present several different theories which show promise of satisfying this transient-response requirement. These same theories are capable of reasonably good representation of the steady shear viscosity at relatively low shear rates, as well as the dynamic viscosity and storage modulus during oscillatory shearing. However, the representation of the steady shear, primary normal stress difference is less accurate. Three such theories are those of Bogue-Chen (Chen and Bogue, 1972), Carreau (1972), and Spriggs (Huppler et al., 1967, and Spriggs, 1965).

To evaluate these relatively new theories, the experi-

mental rheologist must be able to obtain and analyze suitable transient data in addition to the classical steady and oscillatory shear data. Only recently have a limited number of comprehensive sets of data covering the classical and transient types of flow become available. The three theories cited above have been compared with such data in the respective references. Two commonly studied types of transient behavior are time dependent growth of the shear stress and the first normal stress difference $N_1$ at the instantaneous onset of a constant shear rate and the decay of these two parameters after the instantaneous removal of a constant shear rate. While the measurement of the second normal stress difference $N_2$ during steady shearing is, in principle, straightforward (see for instance Miller and Christiansen, 1972), it is only recently that researchers have reached a consensus on its sign relative to $N_1$, and the behavior of $N_2$ during transient conditions has previously not been investigated.

Steady and oscillatory flow data for $N_1$ and $N_2$ were presented in an earlier paper (Christiansen and Leppard, 1974) for the solutions considered here. We presently report the corresponding extensive shear stress and first normal stress difference data for stress growth and decay. These are compared with the predictions of the Bogue-Chen, Carreau, and Spriggs constitutive theories. Furthermore, extensive second normal stress difference data for stress growth and decay were obtained, and the dependence of the normalized second normal stress difference on time is reported.

## CONSTITUTIVE THEORIES

### Bogue-Chen (1972)

This model is in the general class of integral models in which the stress is determined by integrating the strain history over some past time. The model was motivated by the Coleman and Noll (1961) second-order theory of viscoelasticity. The Coleman and Noll theory weights the strains only with respect to how long ago they took place. Bogue (1966) modified this weighting to account also for the amount of deformation the material was subjected to. For reasons of empirical and mathematical tractability, an exponential weighting factor was chosen. Another central idea encompassed in this model is that the effective time constants are a function of the shear rate such that the relaxation times decrease with increase in shear rate.

To fit this model to experimental data, it is necessary to determine the linear relaxation spectrum from oscillatory shear stress data and to determine the remaining constant $a$ by comparison of predicted and experimental apparent viscosity or first normal stress difference-shear rate functions. The complete set of material functions for this model are presented by Leppard (1974).

### Carreau Model (1972)

The Carreau model (1972) is an extension of Lodge's (1964, 1968, 1958) molecular network theories. The basic premise of molecular network theory is that the polymer molecules form a network consisting of segments of various lengths joined by temporary junctions. Lodge chose a kinetic model in which he assumed that all like segments join the network at a constant rate and have the same probability of leaving the network. These theories are very successful in the linear, low shear rate ranges. They predict the correct magnitude and frequency dependency for oscillatory shear stresses but predict an apparent viscosity and first normal stress difference which is not shear rate dependent. In addition, they predict a zero second normal stress difference.

Carreau (1972) chose to remedy these faults by allowing the rate of segment creation and loss to depend on the strain rate. He also defines a discrete relaxation spectrum based on dilute solution theory. Two different models are generated by assuming different forms for the arbitrary memory functions. Only Model B will be examined here, since Carreau (1972) showed this model to be superior in predicting transient phenomena. The material functions for this model are given by Carreau (1972).

### Spriggs Model (1965)

This model is of interest since it is a recent and highly evolved differential model. Differential models are models in which the time dependency is introduced by the differentiation of the rate of strain with respect to time. The Spriggs model (1965) is an extension of the generalized Maxwell model of linear viscoelasticity.

Oldroyd (1950, 1958) modified an original Maxwell theory by introducing a different operator which satisfies the principle of material objectivity. Spriggs then modified this theory further by requiring that the deviatoric stress tensor $\tau_{ij}$ be traceless. The Spriggs theory yields functions for steady and oscillatory shearing and some transient conditions. The material functions are available in the literature (Huppler et al., 1967, and Spriggs, 1965).

### Experimental Apparatus

All of the data reported here were obtained with a Model R-17 Weissenberg rheogoniometer with cone and plate shearing geometry used. A plate 10 cm in diameter and a 4 deg. cone were used throughout. All experiments were conducted at 25 $\pm$ 0.1°C. The temperature was maintained by circulating water from a constant temperature bath through the walls of the constant environment chamber of the rheogoniometer. The experimental temperature was continuously monitored by a thermocouple embedded in the stationary flat plate. Evaporation from the aqueous samples was prevented by circulating appropriately humidified air through the chamber.

Our oscillatory flow results, as well as those of Lee et al. (1970) and Meissner (1972), have shown that axial movement of the platens during transient experiments can lead to erroneous results, particularly with respect to normal force measurements. To minimize errors of this type, the stiffest normal force spring, spring constant = $1.22 \times 10^6$ dyne/$\mu$, and a very stiff torsion bar, spring constant = $2.1088 \times 10^6$ dynes-cm/$\mu$, were used. The spring constants in the normal force direction for the lower platen assembly and total machine compliance were experimentally determined. Their combined spring constant was found to be 0.89 times that of the stiff, normal force spring. The maximum total platen separation including instrument and normal force spring compliances for the transient experiments was 1.44 $\mu$ at a shear rate of 8.62 $s^{-1}$ for the PEO solution. To examine possible effects of this slight movement, a weight equivalent to this normal force was placed on the upper platen with the sample in place. The gap was manually adjusted for this deflection, and after the sample had totally relaxed, the weight was instantaneously removed. The output was a step change of the correct magnitude with no indication of time-dependent behavior. Thus, it is felt that this slight movement did not effect the growth or decay data. No attempt, either manual or with a servo mechanism, was made to adjust for deflection during the transient experimentation. The correct gap was set for the no-shear case and left at that value throughout testing.

The radial stress distribution across the flat plate was measured by four miniature pressure transducers located at approximately equally spaced logarithmic intervals:

1.28, 1.94, 2.88, and 3.80 cm from the center with their pressure sensing diaphragms flush with the plate surface. These transducers are 1 mm in diameter and have sensitivities of 20 to 30 dyne/cm$^2$ in static calibration testing. Olabisi and Williams (1972) used a single flush mounted transducer in a moveable plate.

During all transient testing, the tortional, total normal force, and four transducer signals were recorded simultaneously by a multichannel, continuous trace optical oscillograph. The frequency response of the oscillograph was governed by the fluid damped galvanometers employed and is specified to be DC to 600 $H_z$. The response of the transducers is approximately 10,000 $H_z$. The time base was established by accurate time lines simultaneously recorded with the data traces.

The two test fluids were a 3% solution of polyethylene oxide in a 57% water, 38% glycerine, and 5% isopropyl alcohol solution (PEO) and a 2.5% solution of polyacrylamide in a 50% water and 50% glycerine solution (PAA).

#### Data Analysis

The sign convention employed considers a tensile stress as being positive. All of the transient data presented in this report are normalized with respect to their steady shearing values. The shear stress and first normal stress differences were determined by the classical cone and plate formulas reported earlier (Christiansen and Leppard, 1974). These formulas are particularly simple for the normalized shear stress and normalized first normal stress difference $\overline{N}_1$ parameters, since they reduce to simple ratios of instantaneous oscillograph displacements by the steady shearing displacements.

The transient second normal stress difference $\hat{N}_2$ is, however, somewhat more difficult to analyze. It is possible to select the four measured point stresses, $\hat{\sigma}_{22}(r, t)$, at a given time and then fit these to a slope-intercept equation from which $\hat{N}_2$ could be obtained by either the classical rim or slope/total force method equation. This process could then be repeated to cover the entire time span. However, in practice this procedure would be extremely laborious and prone to error in the regions of rapidly changing stresses. This analysis can be simplified if the assumption is made that the normalized point stresses $\bar{\sigma}_{22}$ for a particular set of experimental conditions are not a function of radial position, that is

$$\bar{\sigma}_{22} = \frac{\hat{\sigma}_{22}(r, t)}{\sigma_{22}(r)} \neq f(r) \tag{1}$$

The validity of this assumption can be easily evaluated by a plot of $\bar{\sigma}_{22}(t)$ at various radial positions.

Using the rim method, we can obtain the normalized second normal stress difference $\overline{N}_2$ directly from Equation (1) by letting $r = R$. Thus, by assumption (1)

$$\overline{N}_2 \equiv \frac{\hat{\sigma}_{22}(R, t)}{\sigma_{22}(R)} = \bar{\sigma}_{22} \tag{2}$$

and $\hat{N}_2$ grows or decays at the same normalized rate as the point stresses. Interesting results can be obtained by applying this to the slope of the point stress distribution $\hat{\psi} = d\hat{\sigma}_{22}/d \ln r$. By writing the slope in discrete form for points 1 and 2

$$\hat{\psi} = \frac{\hat{\sigma}_{22}(r_1, t) - \hat{\sigma}_{22}(r_2, t)}{\ln(r_1/r_2)} \tag{3}$$

and then multiplying and dividing each point stress by its steady shearing value, one obtains

$$\hat{\psi} = \frac{\dfrac{\hat{\sigma}_{22}(r_1, t)}{\sigma_{22}(r_1)}\sigma_{22}(r_1) - \dfrac{\hat{\sigma}_{22}(r_2, t)}{\sigma_{22}(r_2)}\sigma_{22}(r_2)}{\ln(r_1/r_2)} \tag{4}$$

But, by the assumption, Equation (1), the normalized transient stresses are not a function of $r$ and can be factored out of the Equation (4) leaving what is easily recognized as the steady shear slope $\psi$ in discrete form, or

$$\hat{\psi} = \bar{\sigma}_{22}\,\psi \tag{5}$$

which becomes by definition

$$\bar{\psi} = \hat{\psi}/\psi = \bar{\sigma}_{22} \tag{6}$$

Therefore, the normalized slope of the stress distribution also grows and decays at the same relative rate as each individual normalized point stress.

The effect on $N_1$ can be determined by writing the radial component of the equations of motion less the centrifugal force term in a rearranged form:

$$\hat{N}_1 = \hat{\psi} - 2\hat{N}_2 \tag{7}$$

Multiplication and division of each term on the right-hand side by its steady shearing value yields

$$\hat{\overline{N}}_1 = \left(\frac{\hat{\psi}}{\psi}\right)\psi - 2\left(\frac{\hat{N}_2}{N_2}\right)N_2 \tag{8}$$

The two terms in parentheses are by Equations (6) and (2) both equal to $\bar{\sigma}_{22}$. Factoring out $\bar{\sigma}_{22}$ leaves what is readily seen to be the steady shearing $N_1$. Rearranging Equation (8), we get

$$\overline{N}_1 = \frac{\hat{N}_1}{N_1} = \bar{\sigma}_{22} \tag{9}$$

In like fashion, it can be shown that the normalized total normal force obtained by an integration of the point stress distribution is also equal to $\bar{\sigma}_{22}$.

In summary, if the normalized point stress $\bar{\sigma}_{22}$ is not a function of radial position, then the normalized first and second normal stress differences will grow and decay identically with the normalized point stresses. These conclusions, based on the assumptions, have experimental and theoretical implications. For example, they suggest that one need measure stress growth and decay behavior for only the most conveniently measured parameter, say the total normal force, and compute such behavior for the other parameters from steady state data. It will be shown that the presently reported data support assumption (1).

## RESULTS AND DISCUSSION

The results for steady and oscillatory shearing of the two test fluids were reported and discussed previously (Christiansen and Leppard, 1974). In general, all three models represented the steady and oscillatory data for the PEO solution fairly well, with the Bogue-Chen model being slightly better overall. Nevertheless, there are some relatively large differences between the data and the models. The Carreau and Spriggs models were not able to predict the behavior of the PAA solution owing to the steep power law slopes of the apparent and dynamic viscosity curves. Attempts to fit the models to these slopes resulted in predictions with large swings around the desired straight power law slope. This behavior is the result of specifying a discrete relaxation spectrum of the form

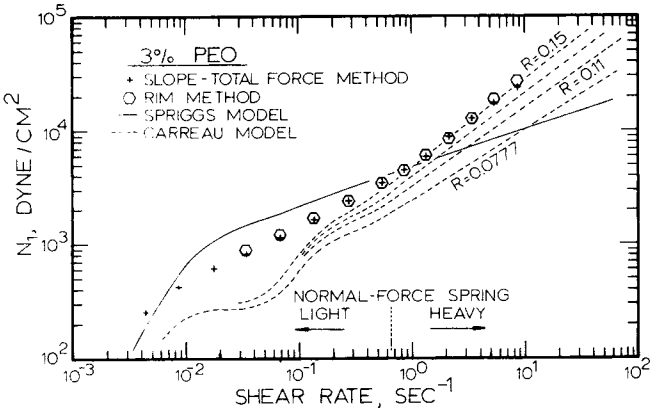


**Fig. 1. Effect of $R$ parameter on first normal stress difference for Carreau model.**

chosen by both Carreau and Spriggs. The Bogue-Chen model was able to accommodate the observed slopes very well. An important weakness of the Bogue-Chen model for both solutions was the necessity of a parameter $a$ for apparent viscosity data different from that for the first normal stress difference data, whereas the theory predicts a single value for both. Even so, there are large discrepancies between the data and the model predictions in some flow conditions.

In fitting the Carreau model to the PEO first normal stress difference data, a value of $R = 0.078$ was determined when the procedure recommended by Carreau (1972) was used. This value yielded a predicted stress difference parallel to but lower in magnitude than the data. A simplified analysis of the effect of this parameter on stress growth shows that this parameter is a major determinant of the time and magnitude of stress overshoot. Therefore, to examine the effect of $R$ on the steady shearing, first normal stress difference and on stress growth, values of 0.11, 0.13, and 0.15 were chosen. The effect on the steady shearing, first normal stress difference is illustrated in Figure 1. As observed, the value of $R = 0.15$ yields a very good representation of the data at the higher shear rates but a very poor representation at lower shear rates. The effect on the shear stress growth appears in Figure 2, where the normalized shear stress growth for a shear rate of 3.43 $s^{-1}$ is presented. The steady shear

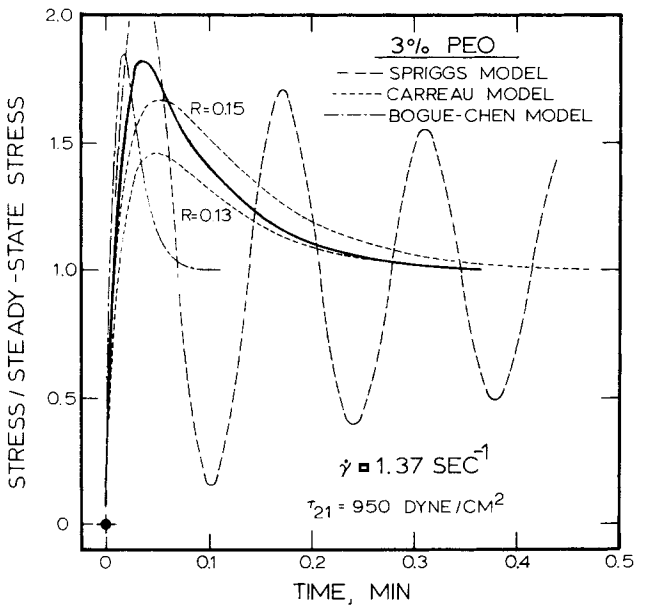


**Fig. 3. Normalized shear stress growth with the predictions of the Spriggs, Carreau, and Bogue-Chen models.**

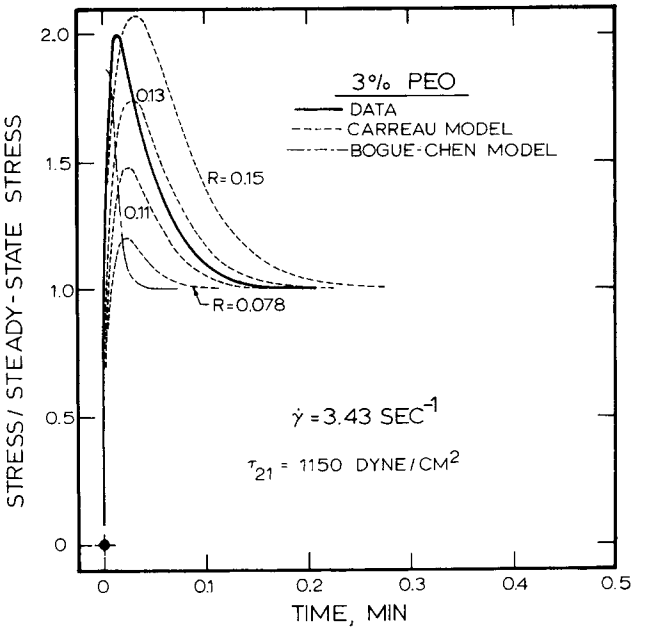


**Fig. 2. Normalized shear stress growth with the predictions of the Bogue-Chen model and of the Carreau model for various values of the parameter $R$.**

stress $\tau_{21}$ was 1150 dynes/cm at this shear rate. This figure shows that larger values of $R$ produce better, but only fair, representations of the observed behavior. The Bogue-Chen representation is for $a = 1.3$, since this value produced the best correlation of the apparent viscosity data. The prediction is very poor, peaking much too soon.

The type of shear stress growth behavior predicted by the Spriggs model is compared with data in Figure 3 for a shear rate of 1.37 $s^{-1}$. Such oscillatory behavior has been reported before by Huppler et al. (1967) and clearly does not describe our shear stress growth data. The Carreau model with $R = 0.15$ and the Bogue-Chen model are at least qualitative representations of the data.

Typical shear stress growths for the PAA solution are shown in Figure 4 for shear rates of 1.37 and 0.544 $s^{-1}$. The Bogue-Chen representations are shown for $a = 1.1$. For both shear rates, the predictions peaked too soon at too great a magnitude. This was generally true for all of

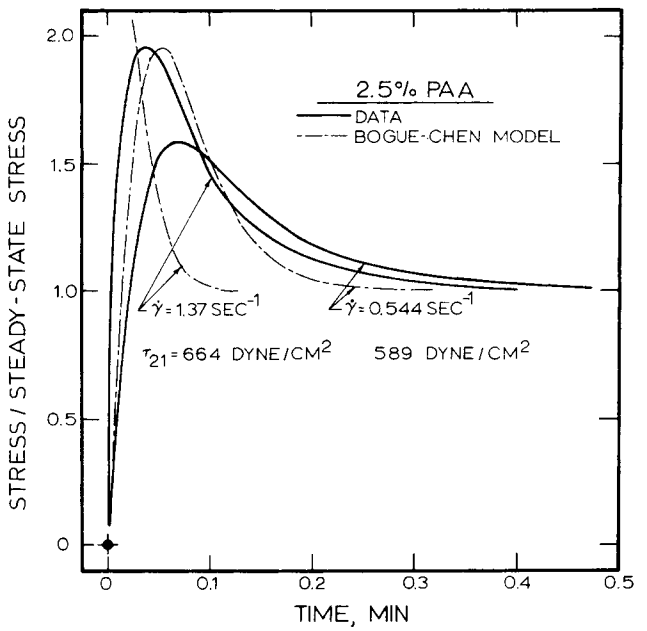


**Fig. 4. Typical shear stress growths for the PAA solution with the predictions of the Bogue-Chen model.**

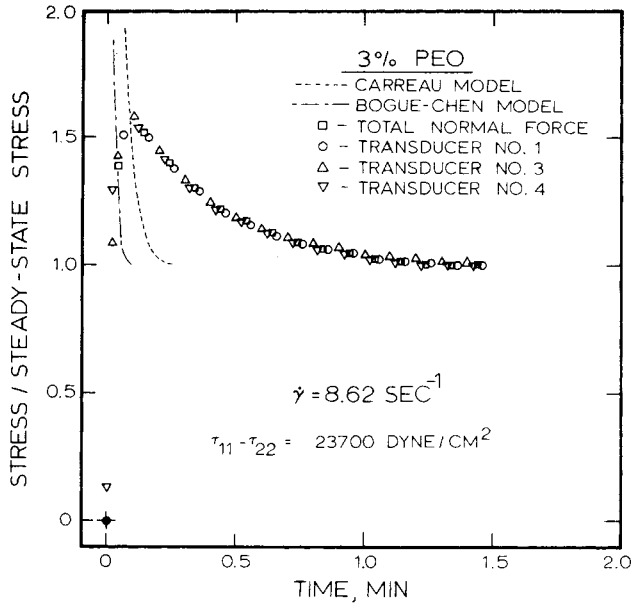


**Fig. 5. Normalized normal stress growth of first normal stress difference and three point stresses.**

the Bogue-Chen representations of shear stress growth.

The shear stress was found to peak sooner and at higher magnitudes as the shear rate was increased, as observed by others (Huppler et al., 1967; Lodge and Meissner, 1973; Meissner, 1972; and Vinogradrov and Belkin, 1965). The peaks, however, did not occur at the same total strain as has been observed by Meissner (1972) and Zapas and Phillips (1971). Rather, the overshoots occurred at larger total strains with increasing shear rates.

To test the assumption that the individual point stresses all grow at the same normalized rate, the normalized stresses indicated by the individual transducers were co-plotted. To generate such plots, the continuous data traces were discretized, and points were plotted at offset time intervals to reduce the data's crowding. Figure 5 shows such a plot for the PEO solution at a shear rate of 8.62 $s^{-1}$. During this run transducer number 2 was inoperative. This plot shows that all normalized point stresses grow at the same normalized rate irrespective of radial position. Also, the normalized total normal stresses are plotted in

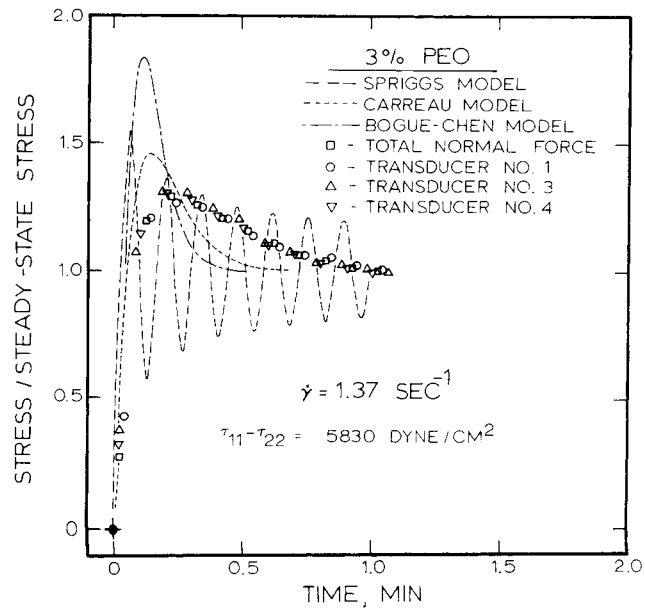


**Fig. 6. Normalized normal stress growth with predictions of the Spriggs, Carreau, and Bogue-Chen models.**

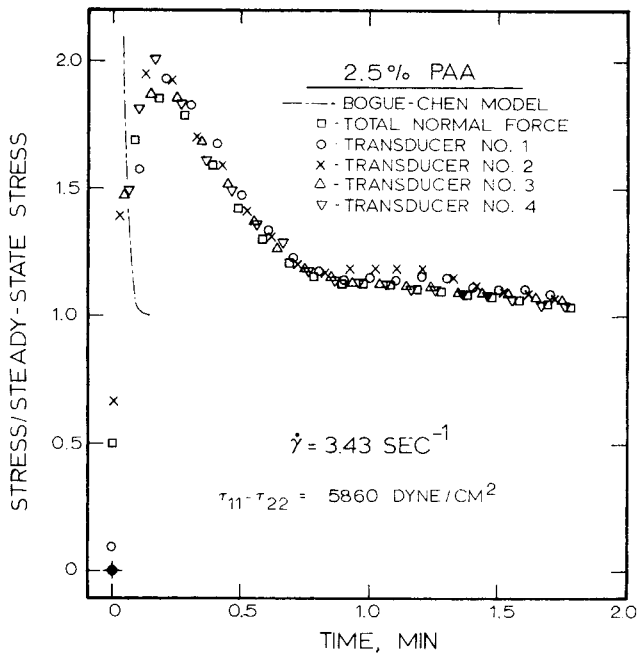


**Fig. 7. Normalized normal stress growth for the PAA solution with the prediction of the Bogue-Chen model.**

Figure 5, and they are coincident with the normalized point stresses. All of the normalized point and total normal stress growth data were coincident for each of the two solutions. Consequently, by Equations (2) and (9), as well as by the linear relation between $N_1$ and the total normal force, the normalized first and second normal stress differences grow at the same rate.

The growth predictions for the Carreau, $R = 0.15$, and Bogue-Chen, $a = 0.5$, models are included in Figure 5. For each model the predicted growth peaked much too soon at too large a magnitude. Figure 6 shows the data and model predictions at a shear rate of 1.37 $s^{-1}$. Again, the peaks for both the Carreau and Bogue-Chen models occur too soon and are too large. In general, the Carreau model, with $R = 0.15$, yielded a somewhat better representation of the normalized normal stress growth than did the Bogue-Chen model.

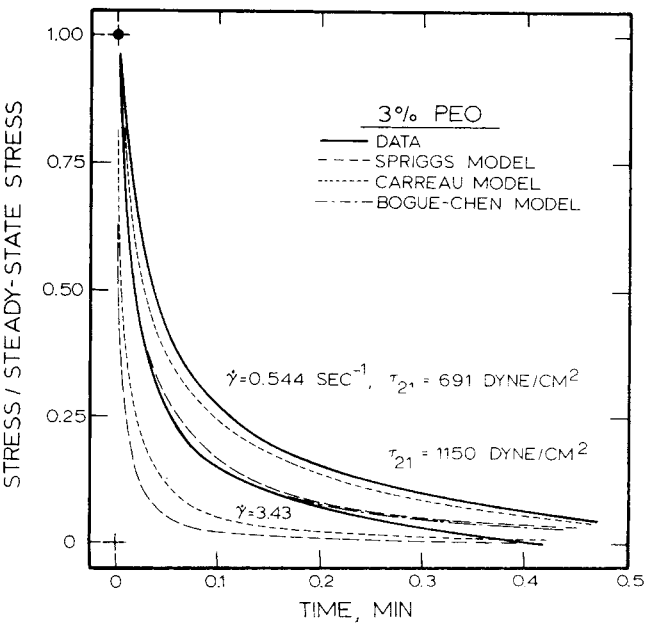


**Fig. 8. Typical shear stress decay with the predictions of the Spriggs, Carreau, and Bogue-Chen models.**

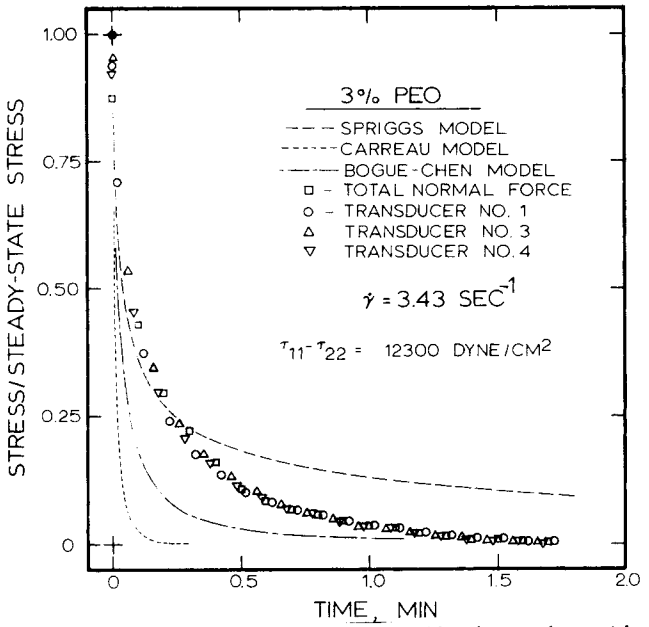


**Fig. 9. Typical normal stress decay for the PEO solution along with the predictions of the three constitutive models.**

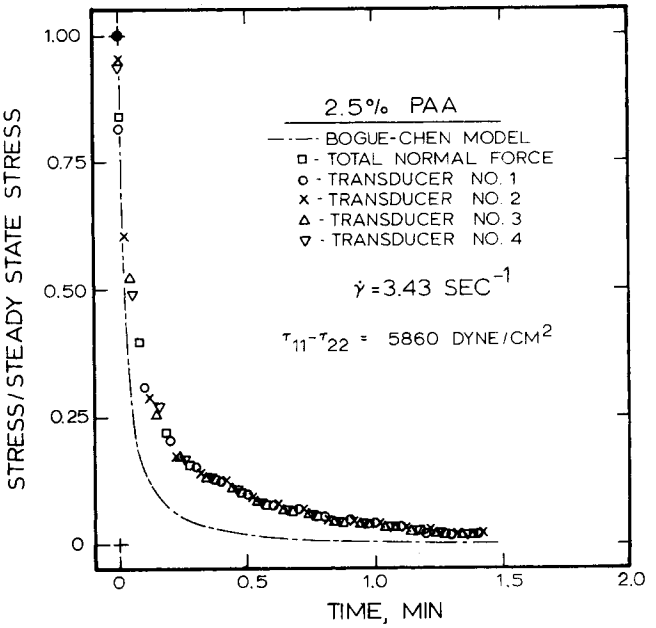


**Fig. 10. Typical normal stress decay for the PAA solution with the Bogue-Chen prediction.**

Figure 7 represents typical normal stress growth data and a prediction of the Bogue-Chen model for the PAA solution. The Bogue-Chen model predicted a much too rapid growth and too large an overshoot magnitude, as was the case at the other shear rates investigated.

For both solutions the magnitude of the overshoot increased, and the time to the maximum overshoot decreased with increase in shear rate. At any given shear rate, the normal stresses developed more slowly and exhibited a lower normalized overshoot magnitude than did the shear stresses. At a shear rate of 0.544 $s^{-1}$, the PAA normal stress did not exhibit any overshoot. For this case the total normal force and point stresses were also coincident.

In no instance for either shear or normal stress growth was there any indication of stress undershoot as has been observed by Chen and Bogue (1972), Huppler et al. (1967), and Lauffer et al. (1973, 1974). However, our shear rates may have been insufficiently high. In all cases where overshoot was observed, the stress would grow, peak, and decrease monotonically to the steady rate value.

Typical shear stress decay curves for the PEO solution are shown together with the predictions of the three models in Figure 8. The Spriggs and Bogue-Chen models yielded almost identical predictions which decayed somewhat faster than the observed data. The Carreau model also predicted a faster decay rate than observed but was a better overall representation of the data. Typical normal stress decay data are shown in Figures 9 and 10 for the PEO and PAA solutions, respectively. For both solutions at all shear rates, the normalized point stresses and total normal force decayed at the same normalized rates, proving the validity of the assumption (1) for normal stress decay. Thus, the first and second normal stresses decayed at the same normalized rate under the conditions of this study. For both solutions the stresses decayed more rapidly with increase in shear rate, and the shear stresses always decayed more rapidly than the normal stresses.

## ACKNOWLEDGMENTS

The financial assistance of a National Science Foundation Research grant and traineeship and the help of the NASA Ames Laboratory, in particular Mr. Grant Coon with the pressure transducers, is gratefully acknowledged.

## NOTATION

$a$ = constant in Bogue-Chen model
$f$ = function of
$N_1$ = first normal stress difference, $\tau_{11} - \tau_{22}$, dynes/cm$^2$
$N_2$ = second-normal stress difference, $\tau_{22} - \tau_{33}$, dynes/cm$^2$
$r$ = radial position, cm
$R$ = radius of flat plate, cm, or constant in Carreau model
$t$ = time, s
$\sigma_{22}$ = normal stress component acting on flat plate, dyne/cm$^2$
$\psi$ = $d\sigma_{22}/d \ln r$
$\dot{\gamma}$ = rate of deformation, $s^{-1}$
$\tau_{ij}$ = components of deviatoric stress tensor, dynes/cm$^2$

**Superscripts**

$\bar{}$ = parameter normalized with respect to steady stressing value
$\hat{}$ = time dependent value of parameter either during stress growth or decay

## LITERATURE CITED

Bird, R. B., Ole Hassager, and S. I. Abdel-Khalilk, "Co-rational Rheological Models and the Goddard Expansion," *AIChE J.*, **20**, 1041 (1974).

Bogue, D. C., "An Explicit Constitutive Equation Based on an Integrated Strain History," *Ind. Eng. Chem. Fundamentals*, **5**, 253 (1966).

Carreau, P. J., "Rheological Equations from Molecular Network Theories," *Trans. Soc. Rheol.*, **16**, 99 (1972).

Chen, I-J., and D. C. Bogue, "Time Dependent Stress in Polymer Melts and Review of Viscoelastic Theory" *ibid.*, 59.

Christiansen, E. B., and W. R. Leppard, "Steady-State and Oscillatory Flow Properties of Polymer Solutions" *ibid.*, **18**, 65 (1974).

Coleman, B. D., and W. Noll, "Foundations of Linear Viscoelasticity," *Rev. Mod. Phys.*, **33**, 239 (1961).

Huppler, J. D., E. Ashare, and L. A. Holmes, "Rheological Properties of Three Solutions, Part I, Non-Newtonian Viscosity, Normal Stresses, and Complex Viscosity," *Trans. Soc. Rheol.*, **11**, 159 (1967).

Huppler, J. D., I. F. MacDonald, E. Ashare, T. W. Spriggs, R. B. Bird, and L. A. Holmes, "Rheological Properties of Three Solutions, Part II, Relaxation and Growth of Shear and Normal Stresses," *ibid.*, 181.

Laufer, Z., "Rheological Behavior of Polymer Solutions Under Various Types of Shear Flow," Doctoral Dissertation, Leiden, Holland (1974).

———, H. L. Jalink, and A. J. Staverman, "Time Dependence of Shear and Normal Stresses of Polyethylene and Poly (Ethylene Oxide) Solutions," *J. Polymer Sci.*, **11**, 3005 (1973).

Lee, K. H., L. G. Jones, K. Pandalai, and Robert S. Brodkey, "Modifications of an R-16 Weissenberg Rheogoniometer," *Trans. Soc. Rheol.*, **14**, 555 (1970).

Leppard, W. R., "Viscoelasticity: Stress Measurements and Constitutive Theory," Ph.D. dissertation, Univ. Utah, Salt Lake City (1974).

Lodge, A. S., "A Network Theory of Constrained Elastic Recovery in Concentrated Polymer Solutions," *Rheol. Acta*, **1**, 158 (1958).

Lodge, A. S., *Elastic Liquids*, Academic Press, New York (1964).

Lodge, A. S., "Constitutive Equations From Molecular Network Theories for Polymer Solutions," *Rheol. Acta*, **7**, 379 (1968).

———, and J. Meissner, "Comparison of Network Theory Predictions with Stress/Time Data in Shear and Elongation for a Low-Density Polyethylene Melt," *ibid.*, **12**, 41 (1973).

Meissner, J., "Modifications of the Weissenberg Rheogoniometer for Measurement of Transient Rheological Properties of Molten Polyethylene Under Shear. Comparison with Tensile Data," *J. Appl. Polymer Sci.*, **16**, 2877 (1972).

Miller, M. J., and E. B. Christiansen, "The Stress State of Elastic Liquids in Viscometric Flow," *AIChE J.*, **18**, 600 (1972).

Olabisi, O., and M. C. Williams, "Secondary and Primary Normal Stresses, Hole Error, and Reservoir Edge Effects in Cone-and-Plate Flow of Polymer Solutions," *Trans. Soc. Rheol.*, **16**, 727 (1972).

Oldroyd, J. G., "On the Formulation of Rheological Equations of State," *Proc. Roy. Soc. (London), Ser. A*, **200**, 523 (1950).

———, "Non-Newtonian Effects in Steady Motion of Some Idealized Elastico-Viscous Liquids," *ibid.*, **245**, 278 (1958).

Spriggs, T. W., "A Four Constant Model for Viscoelastic Fluids, *Chem. Eng. Sci.*, **20**, 931 (1965).

Vinogradov, G. V., and I. M. Belkin, "Elastic Strength and Viscous Properties of Polymer (Polyethylene and Polystyrene) Melts," *J. Polymer Sci.*, **A-3**, 917 (1965).

Zapas, L. J., and J. C. Phillips, "Simple Shearing Flows in Polyisobutylene Solutions," *J. Res. Natl. Bur. Stand.*, **75A**, 33 (1971).

*Manuscript received March 11, 1975; revision received June 5, and accepted June 6, 1975.*

# Prediction of Dynamic Temperature Distributions in the Human Body

**CHARLES E. HUCKABA**
**HAK-SHING TAM**
**ROBERT C. DARLING**
**and**
**JOHN A. DOWNEY**

**Department of Rehabilitation Medicine**
**College of Physicians and Surgeons**
**Columbia University**
**New York, New York 10032**

**A detailed procedure is presented for the calculation of unsteady state temperature distributions throughout the human body. The adequacy of the proposed computation procedure is demonstrated by comparison of calculated and experimental results for studies conducted on subjects exposed to decreasing ambient temperatures. Core temperatures were predicted within ±0.2°C, and average deviations for individual skin temperatures generally were within ±0.5°C.**

## SCOPE

Proposed control mechanisms for use in predicting human thermoregulatory responses to various types of heat and exercise transients can be evaluated only through the use of an acceptable model of the controlled body system.

Computer simulation of the human thermal system would be of value to both engineers and clinicians. The availability of such techniques could provide a rational basis for improving the efficiency of human performance, especially in stressful thermal environments, of production workers, miners, and even be useful in the conditioning of athletes. In the medical field one can envisage a variety of potential applications including the improved management of fevers, better maintenance of body heat balance during surgery, as well as more effective application of heat and exercise modalities in physical therapy regimens prescribed for paralytic patients.

On the other hand, the procedures described in this paper demonstrate generally applicable methods for treating the dynamics of distributed parameter systems having both internal heat generation and partial internal regulation of heat dissipation. Since the operation of large packed bed reactors bears many analogies to such a system, the techniques developed for the physiologic system may well be used to advantage in the analysis of such corresponding technological situations.

The present paper constitutes an extension of our previous work (Huckaba et al., 1973), concerned with steady state temperature distributions, to the dynamic case. Prior developments reported by both a chemical engineer (Wissler, 1970) and a biophysicist (Stolwisk, 1970) also constituted valuable background resources. In neither instance, however, was a comparison provided of computed and experimental values of individual skin temperatures. Comparison of mean skin temperatures constitutes a less critical test of the efficacy of a proposed model than the direct comparison of individual values as provided in this study.

Charles E. Huckaba is with the Engineering Division, National Science Foundation, Washington, D.C. 20550.